

Production ratios for hadrons produced in muon-proton inelastic scattering at 219 GeV

J. Proudfoot,* N. E. Booth, T. W. Quirk,[†] and W. S. C. Williams
Department of Nuclear Physics, The University of Oxford, Oxford, OX1 3RH, United Kingdom

H. L. Anderson, W. W. Kinnison,[‡] H. S. Matis,[‡] L. C. Myriantopoulos,[§] and S. C. Wright
Enrico Fermi Institute and University of Chicago, Chicago, Illinois 60637

W. R. Francis[¶]
Physics Department, Michigan State University, East Lansing, Michigan 48824

B. A. Gordon,^{||} W. A. Loomis, F. M. Pipkin, A. L. Sessoms,** W. D. Shambroom,^{††} C. Tao,^{**} and Richard Wilson
High Energy Physics Laboratory and Department of Physics, Harvard University, Cambridge, Massachusetts 02138

R. G. Hicks^{‡‡}
Department of Physics, The University of Illinois at Urbana-Champaign, Illinois 61801

T. B. W. Kirk
Fermilab, Batavia, Illinois 60510

L. W. Mo
Physics Department, Virginia Polytechnic Institute and State University, Blacksburg, Virginia 24061

A. Skuja
Department of Physics and Astronomy, University of Maryland, College Park, Maryland 20742
 (Received 9 March 1981; revised manuscript received 6 August 1981)

Results on kaon, pion, and proton production in muon-proton scattering are presented for $1 < Q^2 < 80 \text{ GeV}^2$ with an average Bjorken x of 0.033. The measured particle fractions for $z > 0.2$ ($z = P_{\text{had}}/\nu$) are $f_{\pi} = 0.764 \pm 0.028$, $f_K = 0.187 \pm 0.042$, and $f_p = 0.049 \pm 0.013$. The K^{\pm}/π^{\pm} ratios as a function of z and p_T^2 are presented: The ratios increase with z , and with p_T^2 for $z < 0.3$.

In this paper we report measurements on identified charged hadrons produced in the interactions of 219-GeV muons with a hydrogen target. A publication is in preparation on the results for charged-hadron production without particle identification. The data were taken using the muon-scattering facility at Fermilab. The main features of this facility have been described previously,^{1,2} and the results for unidentified-charged-hadron production and for neutral-strange-particle production at 147 GeV have been published.^{2,3} To provide some charged-particle identification a multicell gas Čerenkov counter was added to the downstream spectrometer to provide particle identification and will be described briefly below. The results are based on a total flux of 3.8×10^{10} incident muons yielding 8×10^3 useful events in the kinematic range $1 < Q^2 < 80 \text{ GeV}^2$ and $10 < \nu < 200 \text{ GeV}$ and having $\langle x \rangle = 0.033$ where Q^2 is the square of the four-momentum transfer of the muon and ν its laboratory energy loss, and $x = Q^2/2M\nu$ is the Bjorken scaling variable. The average squared ha-

dron center-of-mass energy $\langle s \rangle$ is 252 GeV^2 .

The position of the Čerenkov counter is shown schematically in Fig. 1. The counter consisted of a gas cell 2.0 m long. Čerenkov light was collected by means of 18 mirrors with dimensions $0.6 \text{ m} \times 1 \text{ m}$ and a radius of curvature 2 m mounted in two rows

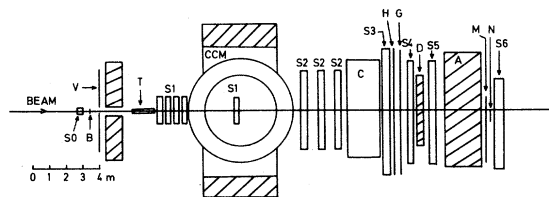


FIG. 1. Diagram showing the layout of the Fermilab Muon Spectrometer Facility. T is the liquid hydrogen target. S_0 and S_1 are multiwire proportional chambers. S_2 – S_6 are multiwire spark chambers. B , V , G , H , M , and N are counter hodoscopes. CCM is a magnet. A and D are absorbers. The Čerenkov counter is marked C .

of nine, one above and the other below the nominal beam position. Each mirror was viewed by a single photomultiplier (RCA 4522) mounted in a Winston cone.⁴ A deadener 35 cm \times 25 cm was inserted in the beam region to prevent light from these particles reaching the mirrors. The multicell assembly was contained in a light-tight box 6 m \times 2.5 m \times 2.6 m deep covered with an opaque Mylar window 0.5 mm thick on the upstream and downstream faces. The mirror thickness was 0.6 g cm⁻². For the data run, the counter was filled with dry nitrogen at atmospheric pressure. The photomultipliers were read out via 10-bit analog-to-digital converters (ADC's) coupled to the anode of each phototube. The ADC's had a full range of 256 pC and their pedestals were set in the range 2–5 pC. A cell was considered lit if its ADC value showed above pedestal.

A single Čerenkov counter does not provide unambiguous particle identification. The momentum thresholds for the emission of Čerenkov radiation by pions, kaons, and protons are shown in Table I. Kaon and proton identification requires a null signal and is therefore dependent on the efficiency of the counter. The mirror edges were determined to ± 0.5 cm by tracking particles through the counter and observing the hit distributions in the cells. The fiducial edges were shrunk inwards from the real edges by 3 cm to remove areas of edge inefficiency resulting from the finite size of the disk of Čerenkov light. Particles falling outside these fiducial boundaries or within the area of the beam deadener or passing more than 80 cm above or below the center edge of the mirror were removed from the analysis. The cell efficiencies were measured using scattered muons and high-momentum tracks, and also estimated from the observed pulse-height distribution. No significant differences were observed between cells. Variation of efficiency with momentum and position in the cell was also investigated and none was observed.

The average inefficiency of the counter for particles with a momentum well above the pion, kaon, and proton thresholds was $(1.93 \pm 0.10)\%$. Attributing all inefficiency to quantum inefficiency, this corresponds

TABLE I. Čerenkov-light emission threshold momenta and momenta for 90% and 95% efficiency in nitrogen at atmospheric pressure ($n = 1.000290$) assuming the average number of photoelectrons from a relativistic particle traversing the Čerenkov counter is 3.95. All values are given in GeV.

Particle	Threshold	90% efficiency	95% efficiency
π	5.8	9.5	12.4
K	20.5	31.4	44
p	38.2	62	78

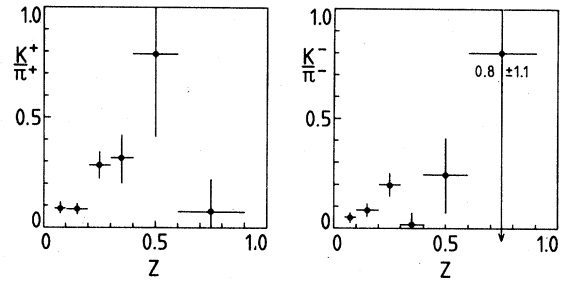


FIG. 2. K^+/π^+ and K^-/π^- ratios as a function of z .

to 3.95 ± 0.05 photoelectrons collected on average from the photocathode. Momentum bands for particle identification were chosen taking into account (1) the threshold smearing due to optical dispersion, (2) the variation of efficiency as the threshold is exceeded, and (3) the possible backgrounds in each band due to misidentification of pions. The bands chosen are shown in Table II. Pions are identifiable in region 2 and protons are separable from pions and kaons in region 4. The average inefficiency in region 2 was measured to be $(3.4 \pm 0.2)\%$ and in region 4 to be $(3.6 \pm 0.2)\%$.

All particle tracks were selected on the basis of the quality of reconstruction and timing. Tracks were reconstructed separately in the bending and nonbending planes upstream of the spectrometer magnet and fully in three dimensions downstream. Cuts on the value of χ^2 of the track fit and on the number of sparks were applied. In addition each track was required to have perfect timing, namely, a hit in all trigger counters pointed at by the track. The scattered muon was identified by its ability to penetrate absorbers D and A , Fig. 1. In this analysis a hadron track was required to link to an upstream track in both planes, and in addition, these links were re-

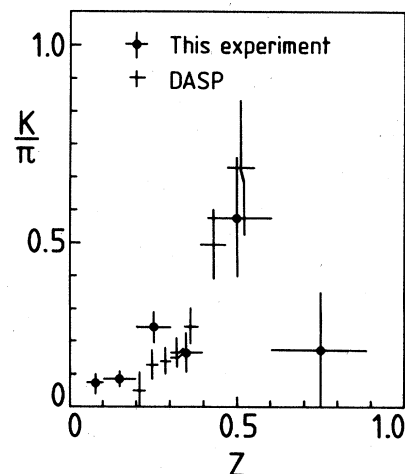


FIG. 3. Ratio $(K^+ + K^-)/(\pi^+ + \pi^-)$ as a function of z as determined in this experiment and from the DASP results of Brandelik *et al.* (Ref. 7).

TABLE II. Particle-identification groups. An entry "undetermined" means a threshold region where the inefficiencies make it impossible to separate particles.

Region	Momentum range (GeV)	Particle classification	
		Radiation observed	No radiation observed
1	5.8–12.4	π	Undetermined
2	12.4–21.2	π	K, p
3	21.2–31.4	Undetermined	Undetermined
4	31.4–38.2	π, K	p

quired to point within three standard deviations of the interaction vertex in the target. The geometrical cuts described above with respect to the Čerenkov counter were applied and the particle classified following the scheme outlined in Table II.

Only hadrons in the momentum regions 2 and 4 could be used in the analysis. In total: in region 2, 1382 hadrons were classified as pions and 295 as either kaons or protons or antiprotons; and in region 4, 384 hadrons as pions or kaons and 29 as protons or antiprotons. Following correction for detection efficiency a measurement of the proton fraction f_p is obtained in region 4 [a charged-particle fraction f_m is defined as $(N_m^+ + N_m^-)/N_{\text{all}}$]. With the assumption that the fragmentation functions depend only on z ($=P_{\text{had}}/\nu$) and are independent of Q^2 and ν (scaling), the fractions f_K and f_π are obtained in region 2 using the measured value of f_p and assuming $f_\pi + f_K + f_p = 1$. The results for $z > 0.2$ are shown in Table III where they are compared with those of Aschman *et al.*⁵ obtained in the reaction

$$e^+e^- \rightarrow \text{hadrons}$$

at $\langle s \rangle = 53 \text{ GeV}^2$. Although the center-of-mass energy is considerably lower than in this experiment the results are in rough agreement.

The assumption that the yields are functions of z alone allows the kaon and pion yields in region 2 to be obtained by subtracting the measured proton yield in region 4. However, the latter measurement was limited by statistics, and the subtraction was made assuming a constant fraction f_p of protons. The particle ratios of K^\pm to π^\pm as a function of z are shown in Figs. 2 and 3. For the ratios for $0.05 < z < 0.1$ we

find $K^+/\pi^+ = 0.09 \pm 0.03$ and $K^-/\pi^- = 0.06 \pm 0.03$. These results are consistent with the two ratios being equal, as would be expected in a quark-fragmentation model. A Monte Carlo calculation based upon the Field and Feynman model⁶ predicts for these ratios a value ~ 0.27 at $z = 0.1$ rising to 0.6 as $z \rightarrow 1$. Figure 3 shows the total K/π ratio as a function of z for this experiment and the same ratio obtained from the results on e^+e^- annihilation of the DASP collaboration at $\sqrt{s} = 5.0$ and 5.2 GeV .⁷ These data also show an increase in the K/π ratio as z increases, in qualitative agreement with Field and Feynman.

These comparisons with e^+e^- annihilation can be made only if the assumption is made that at the low x of this experiment the muon scatters predominantly from sea quarks so that K^+ and K^- production are expected to be equal. The measured π^+/π^- ratio² combined with the data of Fig. 2 are in agreement with this expectation for $z < 0.3$. In an electroproduction experiment at lower energy ($\langle s \rangle = 21 \text{ GeV}^2$), Martin *et al.*⁸ found the K^+/K^- ratio increasing rapidly with z . This is probably due to the fact that closer to threshold K^+ production is kinematically more favorable than K^- production. Our data do not have sufficient precision to determine how the K^+/K^- ratio behaves for $z > 0.3$ at our higher energy.

A limited investigation into the kinematic variation of K to π ratios was made. The average ratios observed in two bins of Q^2 and z are given in Table IV. There is some indication that for K^+/π^+ at least, in addition to an increase with z , there is also an increase with Q^2 .

The corrected particle ratios K^\pm/π^\pm as a function

TABLE III. Particle-ratio results from this experiment and from Aschman *et al.* (Ref. 5) on particle ratios in e^+e^- annihilation.

Particle ratios	This experiment, $\langle s \rangle = 252 \text{ GeV}^2$ $z > 0.2$	Aschman <i>et al.</i> , $\langle s \rangle = 53 \text{ GeV}^2$	
		$0.4 < p < 1.0 \text{ GeV}$ $0.11 < z < 0.27$	$p > 1.0 \text{ GeV}$ $z > 0.27$
f_π	0.764 ± 0.028	0.87 ± 0.01	0.76 ± 0.02
f_K	0.187 ± 0.042	0.12 ± 0.02	0.16 ± 0.03
f_p	0.049 ± 0.013	0.014 ± 0.005	0.07 ± 0.02

TABLE IV. K -to- π ratios in four bins of Q^2 and z .

Q^2 (GeV 2)	z	K^+/π^+	K^-/π^-
1-4	0.1-0.3	0.08 ± 0.03	0.09 ± 0.03
4-80	0.1-0.3	0.16 ± 0.03	0.12 ± 0.03
1-4	0.3-0.9	0.28 ± 0.13	-0.03 ± 0.05
4-80	0.3-0.9	0.52 ± 0.17	0.19 ± 0.11

of P_T^2 in the regions $0.1 < z < 0.3$ and $0.3 < z < 0.9$ are shown in Fig. 4, where P_T^2 is the square of the transverse momentum of the hadron with respect to the virtual-photon axis. At low z an increase in the relative production of kaons to pions with increasing P_T^2 is suggested. A fit of the form $A + BP_T^2$ gave $A = 0.09 \pm 0.03$, $B = 0.13 \pm 0.07$ GeV $^{-2}$ for the ratio of K^+/π^+ and $A = 0.04 \pm 0.03$, $B = 0.12 \pm 0.07$ GeV $^{-2}$ for the ratio of K^-/π^- . The Field and Feynman model⁶ predicts that kaons will have a larger average transverse momentum than the pions. This is because a larger part of the pions come from resonance decays than is the case for kaons, particularly for $z < 0.3$. Thus the K/π ratio should increase with P_T^2 , in qualitative agreement with our observation.

For $z > 0.3$ the errors are too large to draw any conclusions: The K^+/π^+ distribution could be systematically higher than the K^-/π^- distribution and both consistent with being flat.

In conclusion these results show the expected similarities between hadron production in deep-inelastic muon-nucleon scattering and e^+e^- annihilation. These similarities are expected in a quark-fragmentation model. The predictions of such a model for the particle fractions are also in approximate agreement with the observed results.

We would like to thank the staffs of Fermilab, the

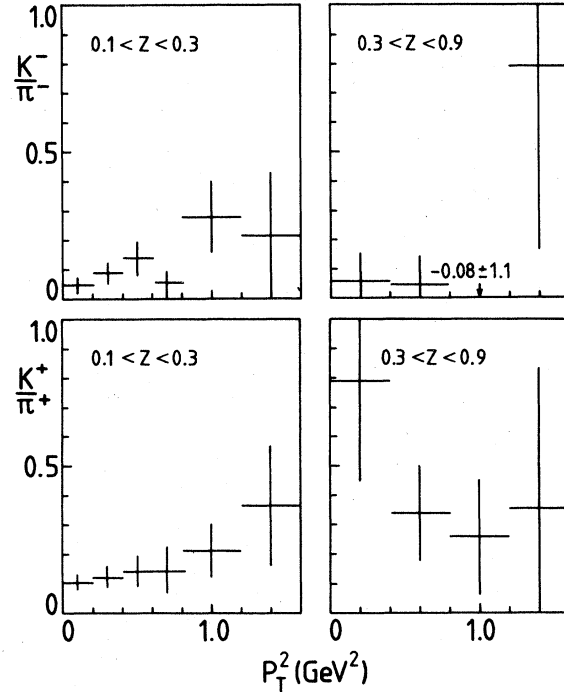


FIG. 4. K^+/π^+ and K^-/π^- ratios as a function of the hadron transverse momentum squared for two regions of z .

Rutherford Laboratory, and our respective laboratories. The U.K. members of this collaboration would like in particular to thank the staff of Fermilab for their hospitality. This work was supported by the National Science Foundation under Contracts No. MPS 71-03-186 and No. PHY-76-23245, by the U.S. Department of Energy under Contracts No. EY-76-c-02-3064, No. E(11-1)-1195, and No. E-(40-1)-2504, and by the Science Research Council (United Kingdom).

*Present address: Rutherford and Appleton Laboratories, Chilton, United Kingdom

† Present address: C.R.A. Services Ltd., Melbourne, Australia.

‡ Present address: Los Alamos National Laboratory, Los Alamos, N.M. 87545.

§ Present address: Department of Physics and Astronomy, University of Maryland, Md. 20742.

¶ Present address: Bell Telephone Laboratories, Naperville, Ill. 60540.

|| Present address: Science Applications, 8400 Westpark, McLean, Va. 22101.

** Present address: U.S. Arms Control and Disarmament Agency, Department of State, 320 21st Street, N.W., Washington, D.C. 20451.

†† Present address: Department of Physics, Northeastern

University, Boston, Mass. 02115.

** Present address: CERN, Ch 1211, Geneva 23, Switzerland.

¶¶ Present address: Department of Physics and Astronomy, Vanderbilt University, Nashville, Tenn. 37235.

¹B. A. Gordon *et al.*, Phys. Rev. D **20**, 2645 (1979).

²W. A. Loomis *et al.*, Phys. Rev. D **19**, 2543 (1979).

³R. G. Hicks *et al.*, Phys. Rev. Lett. **45**, 765 (1980).

⁴H. Hinterberger and R. Winston, Rev. Sci. Instrum. **37**, 1094 (1966).

⁵D. G. Aschman *et al.*, Phys. Rev. Lett. **41**, 445 (1978).

⁶R. D. Field and R. P. Feynman, Nucl. Phys. **B136**, 1 (1978).

⁷R. Brandelik *et al.*, Nucl. Phys. **B148**, 189 (1979).

⁸J. F. Martin *et al.*, Phys. Rev. Lett. **40**, 283 (1978).